8. Selected Reactions of 1st Generation Grubbs Catalyst

8.1. Introduction

1st generation Grubbs catalyst [Ru(=CHPh)Cl_2(PCy_3)$_2$] (Figure 8.1) is moderately stable in solid form compared to other catalysts, like tungsten, molybdenum, tantalum and titanium complexes used for metathesis of alkenes.[1] However, it should still be handled using standard Schlenk techniques due to different reasons, i.e. oxidization by oxygen in solution and moisture. It is thought that the complex forms dimers (bonds between the two ruthenium metal atoms) after the dissociation of the phosphine ligand in solution.[2,3] Thus, the catalyst concentration decreases and low turnover numbers are obtained during the metathesis of olefins. These drawbacks prevent the wide use of the Grubbs catalyst on a large scale for the production of useful, high value olefins from ordinary olefin feedstock in industry.

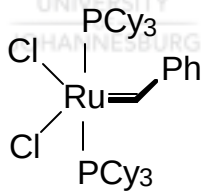

Figure 8.1: 1st generation Grubbs catalyst

The 1st generation Grubbs catalyst [Ru(=CHPh)Cl_2(PCy_3)$_2$], i.e. a benzylidene complex, reacts with excess terminal alkenes to produce the alkylidene complexes [(Cy_3P)$_2Cl_2$Ru=CHR] (R= Me, Et , *n*-Bu, etc.) as kinetic products and upon prolonged reaction times the (Cy_3P)$_2Cl_2$Ru=CH_2 (methylidene) complex as the thermodynamic product. It was found that the methylidene complex decomposes *via* a different

[1] Nguyen, S.T.; Grubbs, R.H., *J. Am. Chem. Soc.* **1993**, *115*, 9858.
[2] Ulman, M.; Grubbs, R.H., *J. Org. Chem.*, **1999**, *64*, 7202.
[3] Amoroso, D.; Yap, G.P.A.; Fogg, D.E., *Organometallics*, **2002**, *21*, 3335.

pathway compared to the other alkylidene complexes (see § 2.3 for a more detailed discussion on these systems).[4]

Different mechanisms have been proposed for the metathesis of olefins by Grubbs catalyst according to the different intermediates that were observed in the kinetic experiments performed in the past[5] and two mechanisms (an associative and a dissociative mechanism) were proposed for the reaction of Grubbs catalyst with alkenes. Subsequent kinetic and mechanistic studies revealed the dissociative pathway as the operative mechanism during alkene metathesis with ruthenium-based alkylidene complexes.[6] It is now generally accepted that the mechanism of both cyclic and acyclic alkene metathesis reactions proceed *via* a series of metallacyclobutanes and carbene complexes. Although the relative stability of the metallacyclobutanes and carbene complexes can change with varying reaction conditions, catalyst composition and alkene substitutions, the mechanism of the alkene metathesis reactions appears to be the same for all catalyst systems. More importantly, results from recent kinetic studies provide no evidence that an associative reaction pathway (involving an 18-electron alkene intermediate) contributes significantly to the metathesis reactions of any of the catalysts.

The following scheme can be constructed to explain the first two steps in the dissociative catalytic cycle (see Scheme 2.3 for the full catalytic cycle), with the first step the dissociation of the phosphine ligand and the second step the coordination of the alkene substrate to the four-coordinate intermediate formed after the dissociation of the phosphine.[4]

[4] Sanford, M.S.; Love, J.A.; Grubbs, R.H., *J. Am. Chem. Soc.*, **2001**, *123*, 6543.
[5] Dias, E.L.; Nguyen, S.T.; Grubbs, R.H., *J. Am. Chem. Soc.* **1997**, *119*, 3887.
[6] Love, J.A.; Sanford M.S.; Day, M.W.; Grubbs, R.H., *J. Am. Chem. Soc.*, **2003**, *125*, 10103.

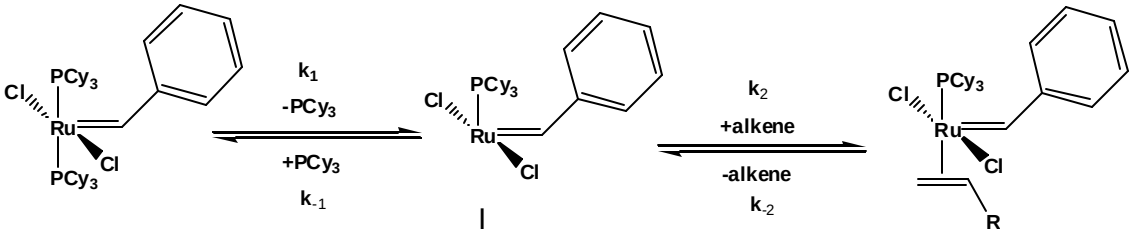

Scheme 8.1: The dissociation of PCy_3 and the coordination of alkene during the first two steps of the metathesis catalytic cycle of 1st generation Grubbs catalyst (also see Scheme 2.3).

As shown in Scheme 8.1, the dissociative substitution of the phosphine ligand by the alkene substrate proceeds through a four-coordinate intermediate (I). Application of the steady-state approximation to I affords the rate expression shown in eq. 8.1. If $k_{-1}[PCy_3] << k_2[alkene]$ (saturation), then eq. 8.1 is reduced to eq. 8.2, and phosphine dissociation becomes the rate-determining step of the reaction.

$$\text{Rate} = \frac{k_1 k_2 [Ru][alkene]}{(k_{-1}[PCy_3] + k_2[alkene])} \qquad 8.1$$

$$\text{Rate} = k_1[Ru] \text{ when } (k_{-1}[PCy_3] << k_2[alkene]) \qquad 8.2$$

8.2. Chemicals and Instrumentation

All the reactions studied during this investigation involved only 1st generation Grubbs catalyst. All reagents used in these experiments were of analytical grade or better. The 1st generation Grubbs catalyst $[Ru(=CHPh)Cl_2(PCy_3)_2]$ was obtained from Sigma-Aldrich. The dichloromethane (DCM) was distilled from phosphorous pentoxide under an argon atmosphere and the benzene was distilled from sodium wire under an argon atmosphere. The 1-octene was percolated through a column of basic alumina (dried at 250 °C beforehand), degassed and stored under argon. Dried dichloromethane or benzene were saturated with the different gases, used as reactants in this study, before each experiment. Standard Schlenk techniques were used to prepare and transfer the stock solutions of the catalyst and different reagents to the cuvettes. The stoppers of the cuvettes were sealed with silicone grease to

exclude any air and moisture from the reactions.

The UV/Vis spectral changes for the slow kinetic reactions were measured on Varian Cary 50 Conc and Varian 100 spectrophotometers with 1.000 ± 0.001 cm path length tandem quartz cells. All the spectrophotometers were equipped with constant temperature cell holders (accurate within 0.1 °C) and Julabo MPV thermostatted water baths (accurate within 0.05 °C) fitted with circulators and the temperatures are reported to within ± 0.1 °C accuracy. The spectrophotometers were coupled with personal computers capable of performing least-squares analyses (Scientist[7]) on the absorption *vs.* time data. The UV/visible spectral changes for the fast kinetic reactions were determined on a Hi Tech SF61DX2 Stopped Flow System with a Cryo Flow Low Temperature Unit attached and the rate constants were determined using the KinetAsyst 3.10[8] software package supplied with the instrument.

The "decomposition" reaction of the catalyst or the reaction with the particular reagent was followed at different reagent concentrations. The absorbance *vs.* time data was fitted to a first order rate equation using the non-linear least-squares program Scientist[7], (see Appendix B.1). The solid lines in the figures represent the calculated values and the individual data points the experimental values. The solid lines in Figure 8.8 and Figure 8.11 represent the experimental data and these data sets were fitted to an exponential equation using the KinetAsyst software[8] to obtain the second order rate constants. Complete tables of k_{obs} *vs.* [L] data used for the particular plots presented in the next section are given in Appendix C.

8.3. Results

8.3.1. "Decomposition" reaction of 1st generation Grubbs catalyst

A stock solution of $[Ru(=CHPh)Cl_2(PCy_3)_2]$ was prepared and time-resolved spectral changes of the decomposition reaction of the catalyst precursor were determined on

[7] MicroMath Scientist Software for Windows, Version 2.0 1, MicroMath Inc., **1995**.
[8] KinetAsyst 3.10 Software Package, Hi-Tech Limited, Salisbury, United Kingdom, **2002**.

a spectrophotometer. Figure 8.2 shows the UV/visible spectral changes of the decomposition reaction of the catalyst precursor with time. Figure 8.3 shows the absorbance *vs.* time change for the decomposition reaction of 1st generation Grubbs catalyst at 340 nm. It can be clearly seen from the plot (Figure 8.3) that there is an initial fast reaction (**A**) that is followed by a much slower second reaction (**B**). The observed rate constants for the reactions were calculated using the least-squares program and the values of the observed rate constants are given in Table 8.1.

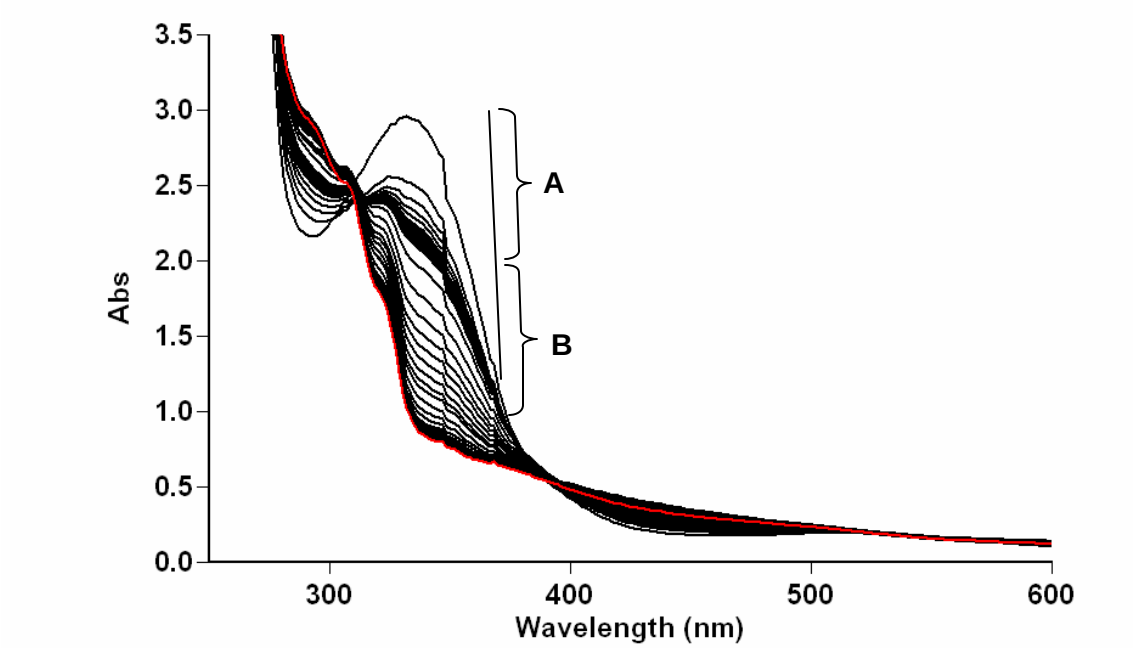

Figure 8.2: Plot of UV/visible spectral change with time for the overall decomposition reaction of $[Ru(=CHPh)Cl_2(PCy_3)_2]$ under a nitrogen atmosphere at 53.0 °C, $[Ru]_T = 3.2 \times 10^{-4}$ M and Δt(A) = 5 min and Δt(B) = 150 min.

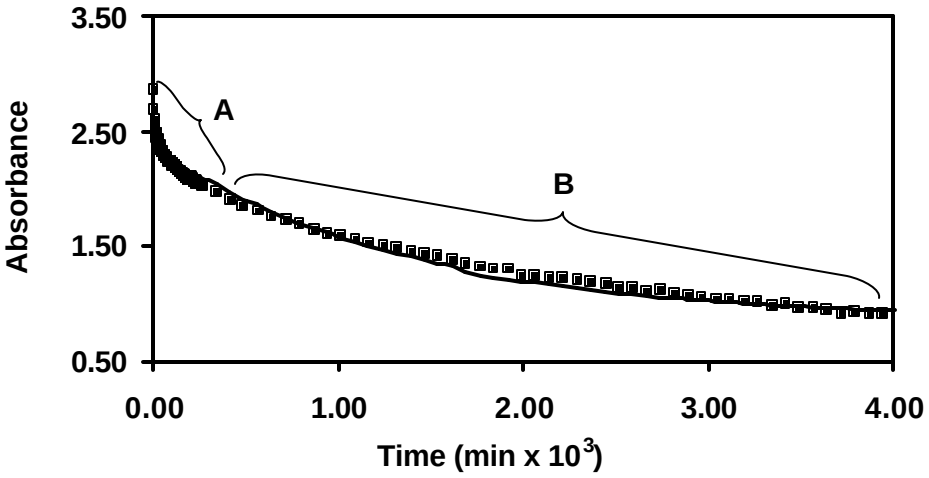

Figure 8.3: Plot of Absorbance *vs.* time for the decomposition reaction of [Ru(=CHPh)Cl$_2$(PCy$_3$)$_2$] in benzene under a nitrogen atmosphere at 53.0 °C, [Ru] = 3.2 x 10^{-4} M and ? = 340 nm.

8.3.2. Reaction of 1st generation Grubbs catalyst with oxygen

A saturated solution of oxygen in dichloromethane was prepared and this solution was used by mixing with dichloromethane under a nitrogen atmosphere to prepare the diluted solutions containing different concentrations of oxygen gas. A stock solution of [Ru(=CHPh)Cl$_2$(PCy$_3$)$_2$] was prepared and 1 cm^3 of the solution together with 1 cm^3 of the particular oxygen solution were placed in a tandem cuvette. Figure 8.4 shows the UV/visible spectral changes over time of the reaction of [Ru(=CHPh)Cl$_2$(PCy$_3$)$_2$] with oxygen and Figure 8.5 shows the absorbance *vs.* time change at 340 nm for the same reaction. The oxygen concentration dependency of the reaction of [Ru(=CHPh)Cl$_2$(PCy$_3$)$_2$] with oxygen gas in dichloromethane is shown in Figure 8.6. The rate constants determined from a least-squares fit of eq. 8.3 and the data in Figure 8.6 are given in Table 8.1.

$$k_{obs} = k_1[L] + k_{-1} \qquad 8.3$$

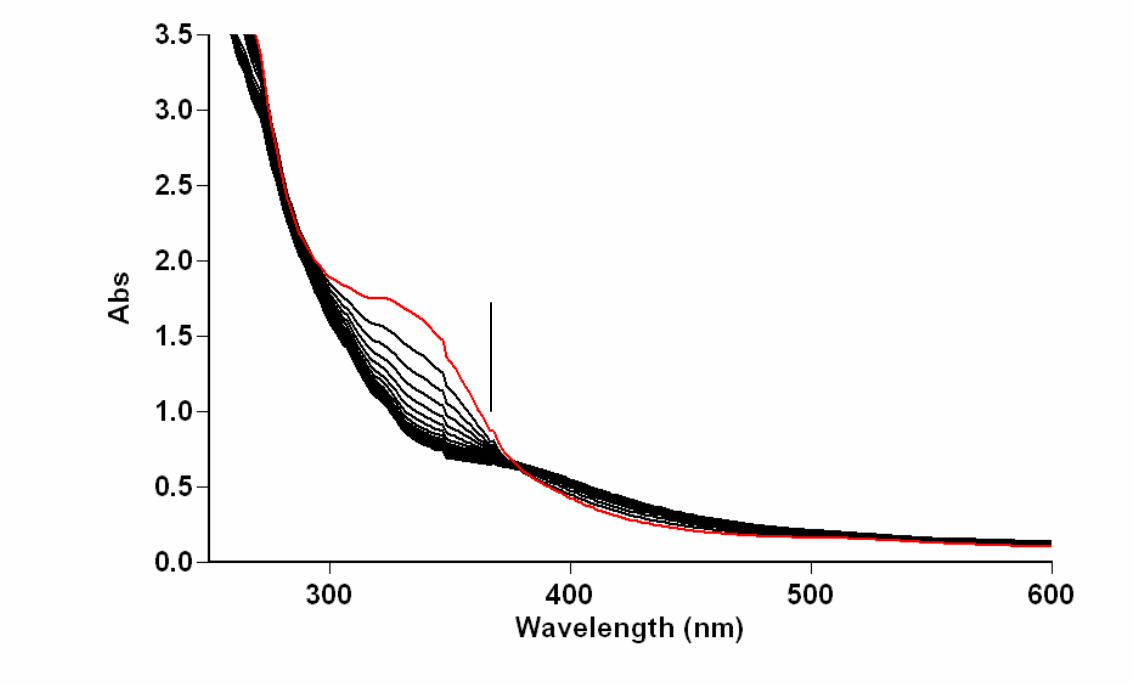

Figure 8.4: **Plot of UV/visible spectral changes for the reaction of $[Ru(=CHPh)Cl_2(PCy_3)_2]$ with oxygen in dry dichloromethane at 25.0 °C, [Ru] = 3.2 x 10^{-4} M, [O] = 0.019 M and Dt = 50 min.**

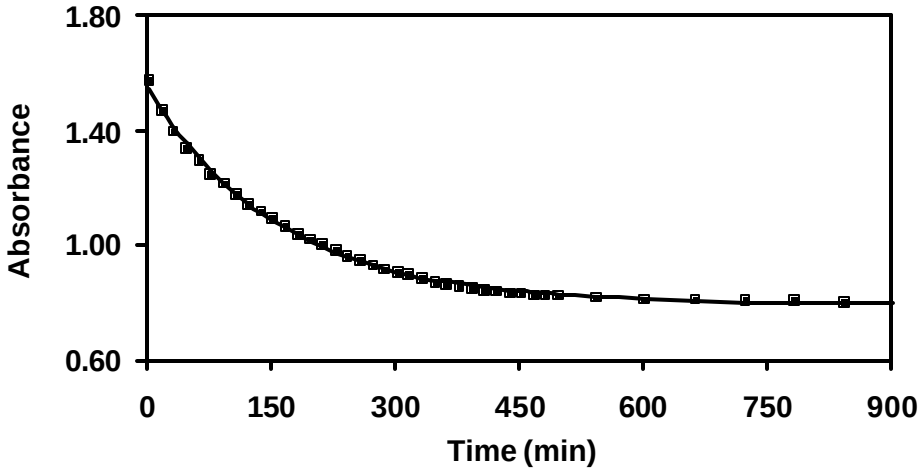

Figure 8.5: **Plot of absorbance *vs.* time change for the reaction of $[Ru(=CHPh)Cl_2(PCy_3)_2]$ with oxygen in dichloromethane at 25.0°C, [Ru] = 3.2 x10^{-4} M, [O] = 0.019 M and ? = 340 nm.**

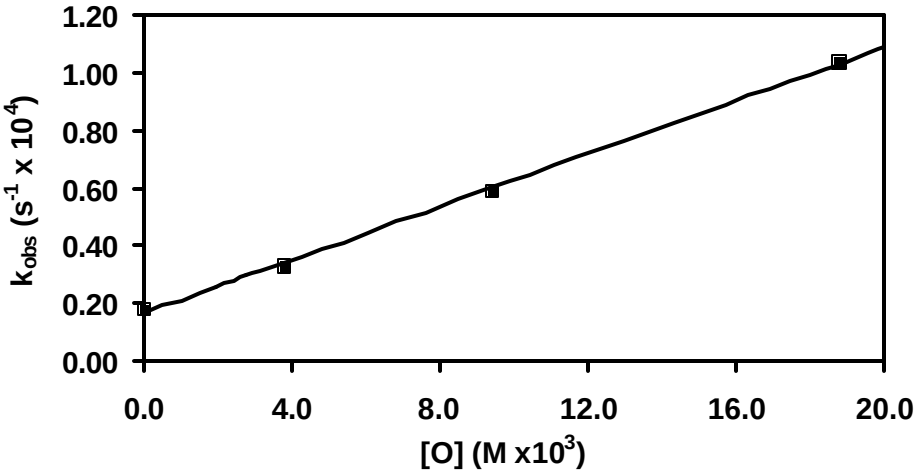

Figure 8.6: Plot of k_{obs} *vs.* [O] for the reaction of [Ru(=CHPh)Cl_2(PCy_3)$_2$] with oxygen in dichloromethane at 25.0 °C, [Ru] = 3.2 x 10^{-4} M and ? = 340 nm.

8.3.3. Reaction of 1st generation Grubbs catalyst with 1-octene

The time resolved UV/visible spectral changes for the reaction between [Ru(=CHPh)Cl_2(PCy_3)$_2$] and a 1-octene/benzene solution are shown in Figure 8.7. The absorbance *vs.* time change for the reaction between [Ru(=CHPh)Cl_2(PCy_3)$_2$] and 1-octene is shown in Figure 8.8 and the effects of temperature and concentration of 1-octene on the observed rate constant are shown in Figure 8.9. The k_{obs} *vs.* concentration of 1-octene data for each of the three temperatures was fitted to a least-squares program[7] to eq. 8.1 and the second order rate constants are given in Table 8.1.

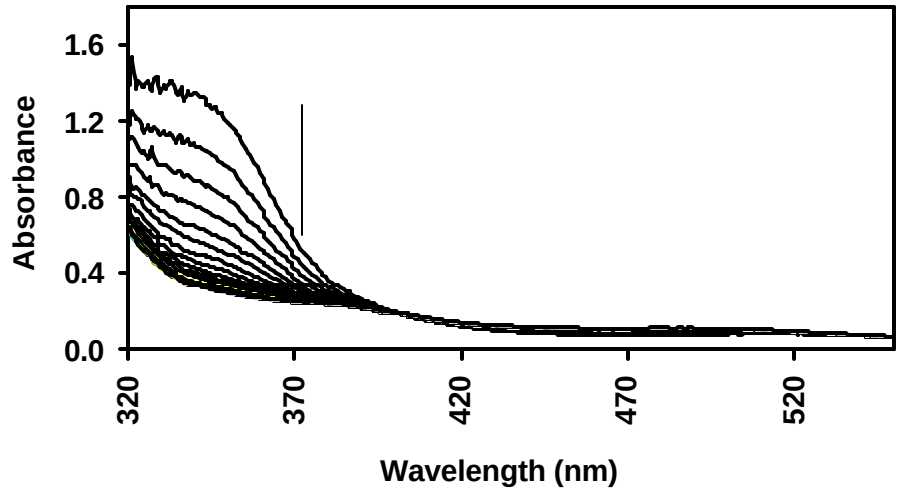

Figure 8.7: Plot of UV/visible spectral change with time for the reaction of $[Ru(=CHPh)Cl_2(PCy_3)_2]$ with 1-octene at 25.0 °C, [Ru] = 1.6 x 10^{-4} M, [1-octene] = 1.6 x 10^{-2} M and Δt = 10 s (stopped-flow).

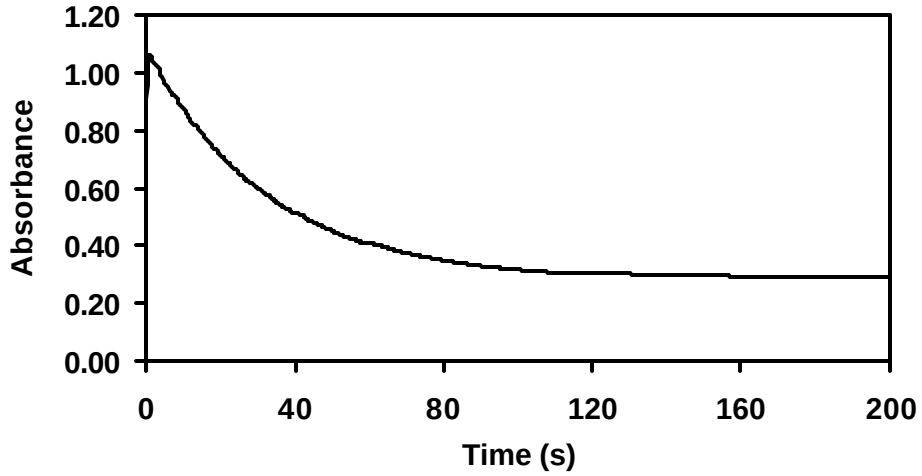

Figure 8.8: Plot of absorbance *vs.* time change for the reaction of $[Ru(=CHPh)Cl_2(PCy_3)_2]$ with 1-octene at 25.0 °C, [Ru] = 1.53 x 10^{-4} M, [1-octene] = 3.2 x 10^{-2} M and ? = 340 nm (stopped-flow).

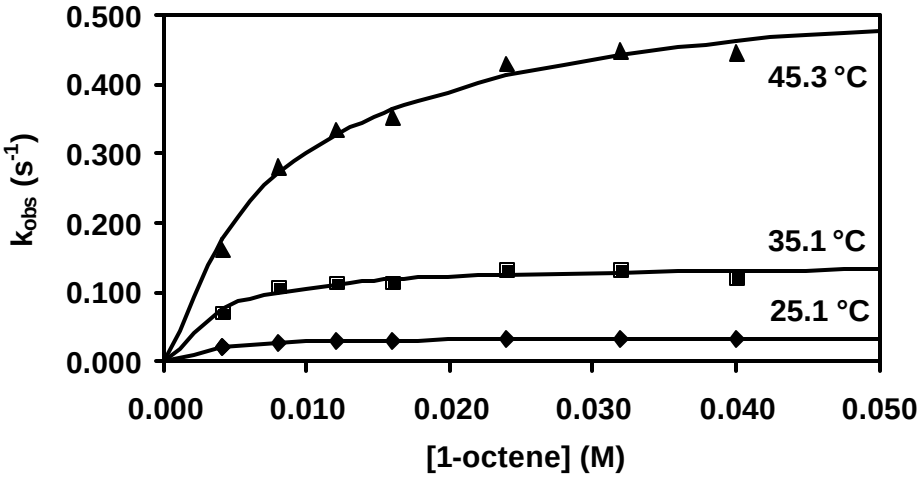

Figure 8.9: Temperature and [1-octene] dependencies of the reaction of $[Ru(=CHPh)Cl_2(PCy_3)_2]$ with 1-octene in benzene, [Ru] = 1.53 x 10^{-4} M and ? = 340 nm.

8.3.4. Reaction of 1st generation Grubbs catalyst with ethene gas

Ethene gas was dissolved in benzene and this saturated solution was used with benzene under an argon atmosphere to prepare ethene/benzene solutions containing different concentrations of ethene. The UV/visible spectral changes of the reaction between $[Ru(=CHPh)Cl_2(PCy_3)_2]$ and ethene were measured on the stopped-flow spectrophotometer (Figure 8.10). The absorbance *vs.* time data for the reaction of $[Ru(=CHPh)Cl_2(PCy_3)_2]$ is given in Figure 8.11 and the ethene concentration and temperature dependencies of this reaction are shown in Figure 8.12. The second order rate constants were calculated from the data in Figure 8.12 and eq. 8.1 using a least-squares program[7] and the values of the rate constants are given in Table 8.1

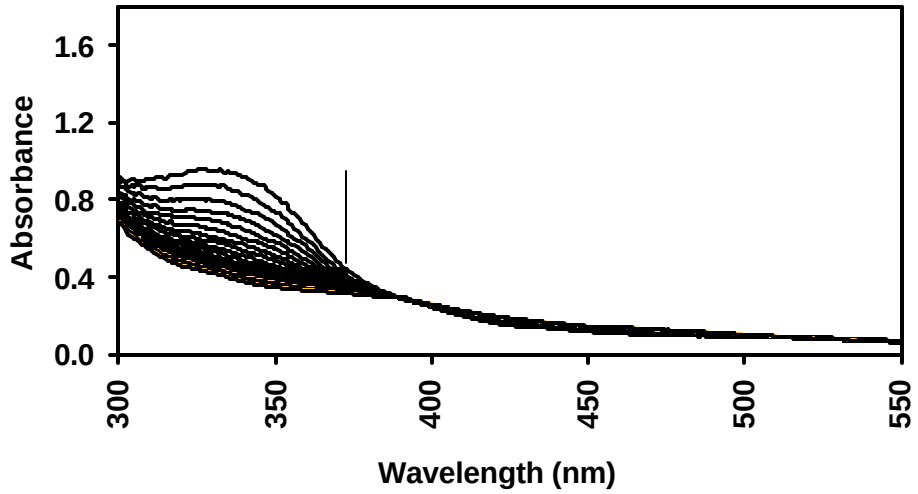

Figure 8.10: Plot of UV/visible spectral change with time for the reaction of [Ru(=CHPh)Cl$_2$(PCy$_3$)$_2$] with ethene gas in benzene at 25.0 °C, [Ru] = 1.6 x 10^{-4} M, [ethene] = 0.14 M, Dt = 4 s (stopped-flow).

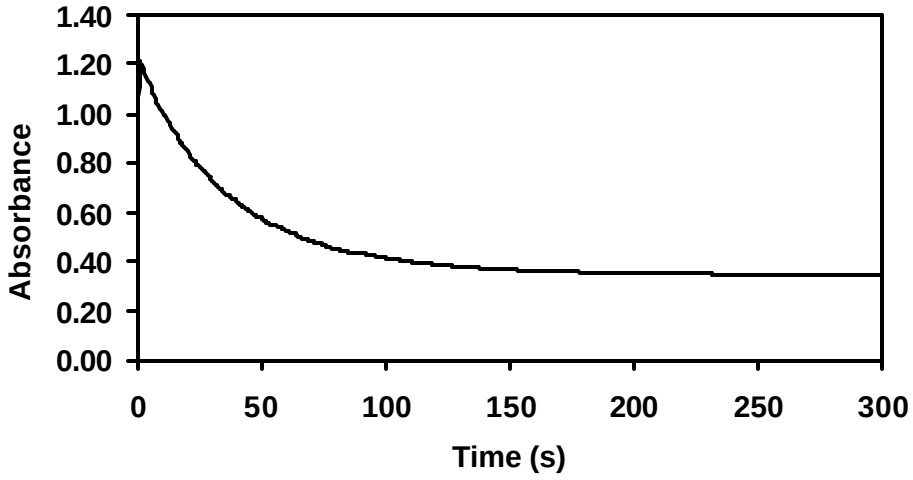

Figure 8.11: Plot of absorbance *vs.* time change for the reaction of [Ru(=CHPh)Cl$_2$(PCy$_3$)$_2$] with ethene gas in benzene at 25.0 °C, [Ru] = 1.53 x 10^{-4} M, [ethene] = 0.143 M and ? = 340 nm (stopped-flow).

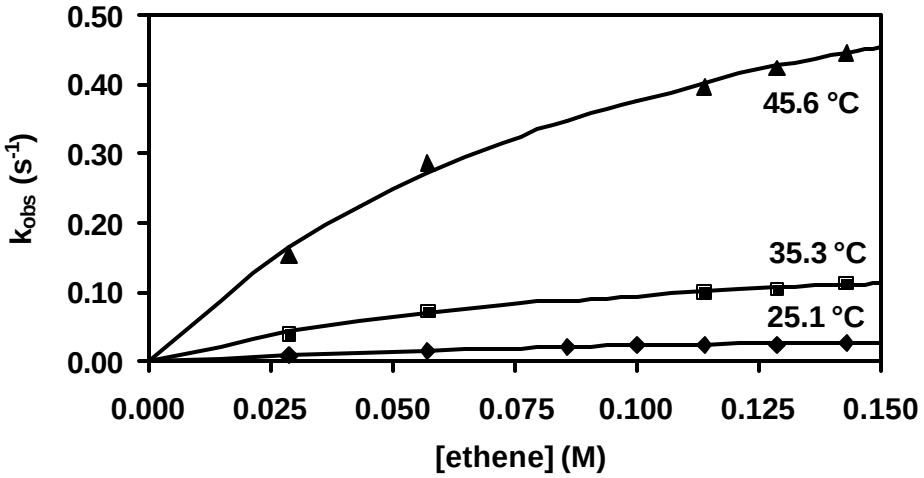

Figure 8.12: Temperature and [C_2H_4] dependencies of the reaction of [Ru(=CHPh)Cl_2(PCy_3)$_2$] with ethene gas in benzene, [Ru] = 1.5 x 10^{-4} M and ? = 340 nm.

Table 8.1: Kinetic data for the reactions of 1st generation Grubbs catalyst under varying conditions and with different reactants.

Constant	Decomposition	Oxygen	1-Octene	Ethene
k_{obs}(overall) (**A** + **B**)	1.52(4) x 10^{-5}			
k_{obs}(0-60) (**A**)	8.5(4) x 10^{-4}			
k_{obs}(60-4000) (**B**)	1.06(2) x 10^{-5}			
25 °C				
k_1 (M^{-1} s^{-1})		4.6(1) x 10^{-3}		
k_{-1} (s^{-1})		1.7(1) x 10^{-5}		
k_1 (M^{-1})			0.40(4)	10(1)
k_2 (s^{-1})			0.0346(6)	0.047(5)
35 °C				
K_1 (M^{-1} s^{-1})			0.29(7)	10(1)
k_2 (s^{-1})			0.143(7)	0.19(1)
45 °C				
k_1 (M^{-1} s^{-1})			0.12(1)	10(1)
k_2 (s^{-1})			0.56(2)	0.77(5)

8.4. Discussion

Recent kinetic studies have shown that a dissociative pathway is the operative mechanism during metathesis reactions of 1st generation Grubbs catalysts, therefore, one of the phosphine ligands has to dissociate during the first step in the reaction scheme (see Scheme 8.1). The dissociation of the phosphine ligand creates an active site and a four-coordinate intermediate is formed in the first step (see Scheme 8.1 and also Scheme 2.3 for the full catalytic cycle). The alkene coordinates to the four-coordinate intermediate in the second step of the catalytic cycle. The first two steps are very important, since any factor that influences these two steps will also influence the rest of the catalytic cycle. The thermal decomposition and the reaction of 1st generation Grubbs catalyst with oxygen as well as the initiation reactions with 1-octene and ethene were therefore studied during the course of this investigation as factors governing catalyst initiation and the entering of the ruthenium complex into the catalytic cycle.

The thermal decomposition reaction of the 1st generation Grubbs catalyst was studied under inert conditions at 53 °C. The plot of absorbance *vs.* time of the decomposition reaction of $[Ru(=CHPh)Cl_2(PCy_3)_2]$ shows two distinct reactions, an initial fast reaction (**A**) and a slower second reaction (**B**) (see Figure 8.3). Similar results concerning the UV/visible spectral changes of $[Ru(=CHPh)Cl_2(PCy_3)_2]$ were obtained during a study of the photochemical reaction of the catalyst by Kunkeley and Vogler.[9] The photolysis of $[Ru(=CHPh)Cl_2(PCy_3)_2]$ leads to the same results as the thermal reaction described above. Kunkeley and Vogler ascribed the fast photochemical reaction they observed to the dissociation reaction of the phosphine ligand from the catalyst. However, the rates obtained for the slower thermal reaction in this study are two orders of magnitude smaller than the rate of the photochemical decomposition determined by Kunkeley and Vogler (see Table 8.2).[9] The products of the thermal and photochemical decomposition of 1st generation Grubbs catalyst have not been fully characterized to date.

[9] Kunkely, H.; Vogler, A., *Inorg. Chim. Acta* , **2001**, *325* , 179.

Table 8.2: Kinetic data for the initiation kinetics, phosphine exchange, decomposition reaction and reaction with oxygen of 1st generation Grubbs catalysts, as well as the 2nd generation catalyst.

Catalyst [a]	T (°C)	1	T (°C)	2	T (°C)	3
k_{init} [b] (s^{-1})	10	1.0(1) x 10^{-3}	0	5.4(5) x 10^{-4}	35	4.6(1) x 10^{-4}
k_B [c] (s^{-1})	10	3.8(6) x10^{-3}	0	1.1(2) x 10^{-3}	35	4(3) x 10^{-4}
k_{init} [d] (s^{-1})	20	1.6(1) x 10^{-2}	20	2.8(2) x 10^{-2}		
k_B [c] (s^{-1})	20	1.6(2) x10^{-2}	20	2.6(3) x 10^{-2}		
k_{init} [e] (s^{-1})	25	3.46(6) x 10^{-2}				
k_{init} [f] (s^{-1})	25	4.7(5) x 10^{-2}				
k_{decomp} [g] (s^{-1})	25	4.1 x 10^{-3} *				
k_{decomp} [h] (s^{-1})	53	1.52(4) x 10^{-5} *				
k_{decomp} [h] (s^{-1})	25	4.6(1) x 10^{-3}				
Ref.		4,9		4		4

[a] 1 = $[Ru(=CHPh)Cl_2(PCy_3)_2]$, 2 = $[Ru(=CH_2CH_2CH_3)Cl_2(PCy_3)_2]$, 3 = $[Ru(=CHPh)Cl_2(PCy_3)(H_2IMes)]$

[b] Initiation reactions of catalysts with ethyl vinyl ether studied by ^{1}H NMR[4].

[c] Rates of dissociation of PCy_3, values predicted for the temperatures from NMR data obtained at 80 °C.

[d] Initiation kinetics of the catalysts with ethyl vinyl ether studied by UV/visible spectroscopy.[4]

[e] Initiation kinetics of the catalysts with 1-octene studied by UV/visible spectroscopy (this work).

[f] Initiation kinetics of the catalysts with ethene studied by UV/visible spectroscopy (this work).

[g] Decomposition reaction of catalyst 1 studied by photolysis.[9]

[h] Decomposition(*) and reaction of catalyst 1 with oxygen studied by UV/visible spectroscopy (this work).

The reaction of the 1st generation Grubbs catalyst with oxygen was studied at different concentrations of oxygen in dichloromethane at room temperature (see § 8.3.2). The plot of absorbance *vs.* time for the reaction of the catalyst precursor with oxygen showed that the reaction is first order (see Figure 8.5). A recent study on the degradation of the 1st generation Grubbs catalyst with primary alcohols, water and oxygen showed that one of the decomposition products was $[Ru(Ph)Cl(CO)(PCy_3)_2]$,[10] which was isolated in 6% yield from a toluene solution of 1st generation Grubb's catalyst reacted with dry air. It was also found that the reaction

[10] Dinger, M.B.; Mol, J.C., *Organometallics*, **2003**, *22*, 1089.

of oxygen with the catalyst precursor occurred in solid samples as well. Unfortunately, the rates of the reaction of $[Ru(=CHPh)Cl_2(PCy_3)_2]$ with oxygen was not determined and the mechanism of the reaction of the catalyst precursor with oxygen was not elucidated in the course of the mentioned study.[10] The rate of the reaction of $[Ru(=CHPh)Cl_2(PCy_3)_2]$ with oxygen is much faster compared to the thermal decomposition reaction of the catalyst precursor (see Table 8.2).

The rate of initiation of the $[Ru(=CHPh)Cl_2(PCy_3)_2]$ complex with 1-octene was determined on a 3rd generation stopped-flow spectrophotometer. The reaction was monitored at 340 nm, the wavelength at which the disappearance of the starting complex $[Ru(=CHPh)Cl_2(PCy_3)_2]$ could be monitored. The reactions of $[Ru(=CHPh)Cl_2(PCy_3)_2]$ with 1-octene showed clean first-order fits of the absorbance *vs.* time data (Figure 8.8). The initiation rate constant was determined as a function of 1-octene concentration, with plots of k_{obs} *vs.* [1-octene] at three different temperatures is shown in Figure 8.9. As expected for a dissociative mechanism (eq. 8.1), k_2 becomes independent of [1-octene] at high concentration where k_2[1-octene] becomes much larger than $k_{-1}[PCy_3]$. The above-mentioned UV/visible results as well as results obtained during previous kinetic studies[4,5,6] confirm that dissociative substitution of one phosphine ligand for the alkene substrate is the operative initiation pathway.

The rate of initiation of the $[Ru(=CHPh)Cl_2(PCy_3)_2]$ complex with ethene was also determined on a 3rd generation stopped-flow spectrophotometer at 340 nm to determine if the initiation rates were similar for sort and long chain alkenes. At this wavelength the disappearance of the starting complex $[Ru(=CHPh)Cl_2(PCy_3)_2]$ was followed, since the absorbance change was the largest compared to the changes at other wavelengths. Fits of the absorbance *vs.* time plots showed that the reaction of $[Ru(=CHPh)Cl_2(PCy_3)_2]$ complex and ethene was also first order and only one reaction was detected. In this case a dissociative mechanism was also confirmed by the fact that k_2 became independent of the concentration of the ethene at high concentrations. The values obtained for the k_2 of both the reactions of $[Ru(=CHPh)Cl_2(PCy_3)_2]$ with 1-octene and ethene are the same within experimental error and the initiation rates of both short and long chain alkenes are the same.

The k_2 values obtained during this investigation of the initiation reactions of $[Ru(=CHPh)Cl_2(PCy_3)_2]$ with 1-octene and ethene compare well to the value found for the initiation reaction of the complex with ethyl vinyl ether by Sanford et al.[4] (see Table 8.2). The k_2 rate constant represents the reaction of the alkene ligand with the four-coordinate intermediate (I) formed by dissociation of the phosphine ligand from the complex (see Scheme 8.1). Sanford et al. chose ethyl vinyl ether as the coordinating ligand, because the metathesis reaction is quenched after the reaction with this alkene (see Scheme 2.3). Previous kinetic studies[4,5,6] have also shown that the values of the initiation rates of the reactions of $[Ru(=CHPh)Cl_2(PCy_3)_2]$ with different alkenes at saturation are identical to the predicted values for the dissociation of the phosphine ligand, within the error of the two measurements (see Table 8.2). However, it is difficult to explain the large difference in k_1 values obtained for phosphine dissociation in the reaction of $[Ru(=CHPh)Cl_2(PCy_3)_2]$ with 1-octene and alkene at this stage (see Table 8.1).

The reactions of the $[Ru(=CHPh)Cl_2(PCy_3)_2]$ complex with 1-octene and ethene are much faster compared to the reaction of the complex with oxygen and even more than two orders of magnitude faster than the decomposition reaction. This implies that the complex has a large scope to be used in the laboratory, but the decomposition and the reaction with oxygen are drawbacks that prevent this type of catalyst precursor to be used on an industrial scale where continuous processes are preferred. However, the values of the different reactions rates that were determined during the course of this study gave valuable information concerning the decomposition, oxidation and initiation of the catalyst with respect to the first two steps of the metathesis cycle of $[Ru(=CHPh)Cl_2(PCy_3)_2]$ and factors governing catalyst entry into the cycle.